lubricants

MDPI

Article

Tribocorrosion Evaluation of Nb_2O_5, TiO_2, and Nb_2O_5 + TiO_2 Coatings for Medical Applications

Giovany Orozco-Hernández [1,*], Pablo Guzmán Durán [2] and William Aperador [3]

[1] Dirección de Posgrados, Universidad ECCI, Cra 19 No. 49-20, Bogotá 110211, Colombia
[2] School of Engineering, Griffith University, Brisbane, QLD 4077, Australia; pablo.guzmanduran@griffithuni.edu.au
[3] Departamento de Ingeniería, Universidad Militar Nueva Granada, UMNG, Bogotá 110111, Colombia; william.aperador@unimilitar.edu.co
* Correspondence: gorozcoh@ecci.edu.co; Tel.: +57-311-792-0209

Abstract: Materials used in biomedicine for purposes of long-time stay inside the body presents diverse sort of problems like cytotoxicity, wear, biocompatibility, and ion liberation along time. This paper presents the characterization of corrosion-wear combined phenomena on Nb_2O_5, TiO_2, and Nb_2O_5 + TiO_2 coatings with future applications as biomaterials. After the films' production process using magnetron sputtering technique, they were characterized through an optic, scanning electron, and atomic force microscopy to evaluate their morphology, structure, and surface damage suffered by the synergy between wear and corrosion phenomena. The life in service of the implant was evaluated in terms of the coating behavior against inside body conditions like charge, wear, and electrochemical degradation. This test was made with electrochemical measurements in simulated biological fluid combined with the wear characterization implementing a potentiostat and a tribometer in a linear wear configuration with a bone pin. As a result, the different electrochemical responses of the films were evidenced by polarization curves and equivalent circuits of the systems. The coefficient of friction and surface degradation were also obtained and evaluated. Comparing the properties of the systems, we conclude that TiO_2 coatings have better behavior in terms of the wear-corrosion synergy phenomena while the systems with Nb present pitting corrosion.

Keywords: tribology; corrosion; biomaterials; surface modification

Citation: Orozco-Hernández, G.; Durán, P.G.; Aperador, W. Tribocorrosion Evaluation of Nb_2O_5, TiO_2, and Nb_2O_5 + TiO_2 Coatings for Medical Applications. *Lubricants* **2021**, *9*, 49. https://doi.org/10.3390/lubricants9050049

Received: 28 February 2021
Accepted: 15 April 2021
Published: 1 May 2021

1. Introduction

One of the most used alloys in implants is Ti6Al4V due to its excellent mechanical and biocompatibility properties, however, recent studies have demonstrated that ions liberation of elements like Al, Ni, Fe, V, and Co could affect cells and generate adverse biological factors that deteriorate the cell's metabolism at long term, thus causing cells death [1,2]. According to this, studies of alloys based on niobium and titanium have turned of high importance as biomaterials components in recent years. Different studies have demonstrated that the addition of these elements as biomaterials enhances properties as Young modulus, ductility, fatigue strength, high hardness, and better corrosion resistance [3–6]. Nevertheless, the acquisition and production of these materials are quite expensive, and in Third World countries, the coverage of all the population is almost impossible due to the reduced funds [2]. Physical vapor deposition (PVD) process can enhance the features of a material as the durability, costs, and effectiveness; thus, it is important to take into account the process costs against the fabrication of an original uncoated piece. Some aspects regarding the advantages of PVD process are the price of the entire equipment, the yield and confidence of the system, capacity of production by hour, labor force and public services, frequency of preventive maintenance, useful life of equipment among others like dimensions of the piece to coat and increase service life of the coated part [7]. Additionally, PVD technology is more ecological in comparison with traditional electroplating [8]. Latchford stablish

that a yield of 1000 discs of data storage coated per hour with coatings ranging from 1 to 200 nm can be achieved by an approximate cost of 30 cents per part [7]. As stablished by Ibrahim et al. PVD coatings have been studied by several researchers in the biomedical application field. This sort of technique offers high purity, high density in the coatings, excellent adhesion strength with the substrate, and smooth surfaces with roughness in the range of the nanometers [9]. Because of that, it is attractive to develop low-cost materials with a similar or better response inside the human body.

As a short-term solution, AISI 316LVM stainless steel presents interesting mechanical properties and a is a low-cost material, however, in terms of electrochemical phenomena acting on its surface, it produces, at medium term, corrosive processes, ions liberation, pitting, and degradation among others causing inflammatory processes and adverse reactions like tissues necrosis, cytotoxicity, and damage inside the human body [10–12]. Coating traditional materials is a standard engineering process that establishes a low-cost solution covering the mandatory regulations in the field. Coatings of Nb_2O_5 and TiO_2 have been widely investigated as biomaterials and have presented excellent results due to the generation of good adhesion with different kind of hard and soft tissue cells as well as high bioactivity [2,13]. Applying this coating by sol–gel or magnetron sputtering techniques plays an essential role in the evaluation of the osseointegration with bone cells, cytotoxicity, cells surface growth process, and antibacterial properties [14–16]. A considerable amount of literature has been published on this kind of coating; however, these studies have not reported an important number of studies concerning the synergy between wear and corrosion that are the leading cause of the degradation in implanted materials. This study aims to investigate the simultaneous phenomena of wear and corrosion that affects the Nb_2O_5, TiO_2, and Nb_2O_5 + TiO_2 coatings surface.

2. Materials and Methods

2.1. Thin Films Deposition

The TiO_2, Nb_2O_5, and Nb-Ti-O thin films were deposited with non-reactive and reactive magnetron sputtering on AISI 316LVM steel substrates using an AJA-ATC 1800 system (AJA International INC, 809 Country Way, N Scituate, MA 02066, USA) with a base pressure of 10^{-7} Pa. Prior the deposition of the films, the stainless-steel substrates were polished through a series of abrasive paper of different grades. Finally, 0.3 μm alumina particles in suspension were used to reach mirror-like aspect. Figure 1 shows an AFM (atomic force microscopy) image of the surface after the preparation process, with an average surface roughness of 500 nm. Subsequently, the substrates were cleaned with isopropanol and acetone before introducing them to the reaction chamber [17,18]. The Nb_2O_5 films were grown in a reactive configuration applying a RF (radio frequency) power of 200 W to the Nb target (AJA International-USA 99.95% pure and 2 in diameter) at gas mixtures of Ar:O_2 = 50:5 (High-purity Ar (99.999%) and O_2 (99.999%)), keeping the total deposition pressure at 0.8 Pa. The TiO_2 films were deposited in a non-reactive configuration, the target used was Ti (99.97% purity and 2 in diameter) applying a RF power of 210 W to the Ti target at gas mixtures of Ar:O_2 = 1:4. The mixtures of titanium and niobium oxides were deposited at a temperature of 300 °C, RF power 50 W, and Ar:O gases relation of 1:4 in volume.

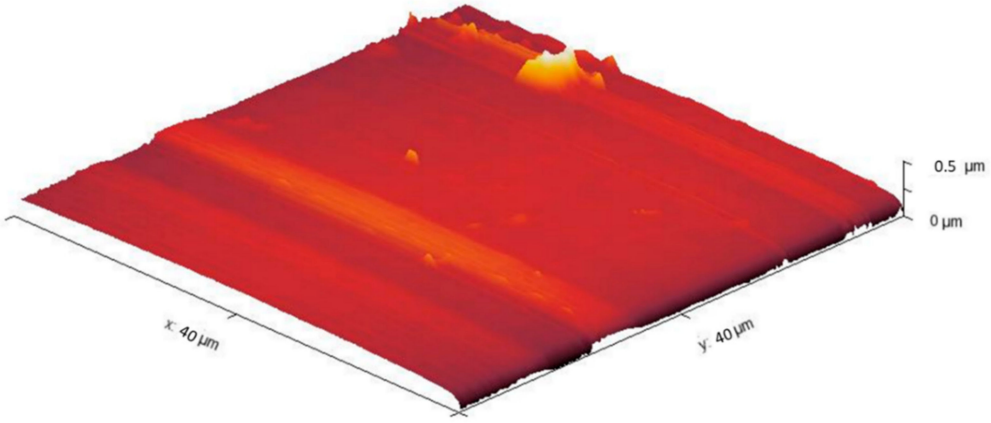

Figure 1. Atomic force microscope (AFM) image of the uncoated substrate surface, after being polished.

2.2. Morphological and Surface Characterization

The scanning electron microscopy technique (SEM-NeoScope JCM-5000, JEOL, Tokyo, Japan) was used to characterize the surface morphology and the synergic effects of wear and corrosion on it. The images were taken at 30× and 300×. Moreover, an atomic force microscope (AFM) was employed to check the surface of the samples, and a stylus profiler was used to measure the wear track generated by the tribocorrosion test.

The surface roughness (R_a) of the specimens was measured by AFM, A Nanosurf EasyScan 2 AFM apparatus (ST Instruments, Liefstal, Switzerland). The surface R_a value shown was calculated as follows: the tip of the sensor inside the equipment traveled on a linear course along the surface of the sample and moved up and down while passing the unsmooth parts of it. These movements along the course as the altitude were then multiplied by the length of it and changed into the area and added together. This was, in turn, divided by the length of the course where the answer gives a number known as R_a.

2.3. Wear-Corrosion

Tribocorrosion experiments were conducted using friction tests on a tribometer with linear reciprocating movement and sphere-plate geometry using pairs of bone pin (cylindrical with spherical tip with 6 mm in diameter) and Nb_2O_5, TiO_2, and Nb2O5 + TiO2 coatings. To establish the duration of the test, the average distance traveled by patients undergoing hip arthroplasty was considered. To determine this distance, it was essential to establish the sliding arch in the femoral head. According to studies, on average, patients who undergo this type of intervention are elderly patients. It is estimated that during their recovery, they travel about 500 m per day [19].

Regarding wear phenomena, a Nanovea T50 tribometer (Nanovea, Irvine, CA, USA), was used in the lineal wear configuration to simulate the cyclic movements of a hip or shoulder joint. The parameters implemented for these tests are summarized in Table 1, and the scheme model of the equipment in Figure 2. These parameters are based on an average person gait.

The tests were carried out in aerated Ringer's physiological solution composed of 9 g/L NaCl, 0.4 g/L KCl, 0.17 g/L $CaCl_2$, and 2.1 g/L $NaHCO_3$ applying a constant load of 5 N with an oscillation frequency of 1 Hz. The length traveled by the pin in each cycle was 10 mm, with the total time test being 60 min, and the pressure contact expected was on the order of 130 MPa. The average coefficient of friction (µ) and the wear coefficients of both the sphere and the coating have been determined.

A vital aspect of this research is the influence of the synergy between wear and corrosion; thus, the tribocorrosion test was made using a temperature of 37 ± 0.2 °C (average body temperature). The tribometer was adequated with an electrochemical cell consisting of a series of three electrodes, i.e., the reference (Ag/AgCl), the counter electrode (platinum wire), and the sample acting as the work electrode. The samples were

isolated with a sample case to exposed the coating with an area of 1 cm^2 as shown in Figure 2. A Gamry potentiostat Model No. PCI 4/750, Warminster, Pennsylvania, USA with the technique of electrochemical impedance spectroscopy (EIS) and potentiodynamic polarization curves was used for the evaluation of corrosion resistance. The polarization curves were measured with a scanning rate of 1 mV/s, in a range of voltages from −350 mV to +350 mV concerning the corrosion potential (E_{corr}). The values of corrosion current densities (i_{corr}) and corrosion potentials were obtained from the polarization curves by extrapolating the cathodic and anodic branch to the corrosion potential (Tafel extrapolation method). The Nyquist diagrams were obtained by sweeping frequency between 0.001 Hz and 100 kHz and using the amplitude of the sinusoidal signal of 10 mV. To increase the reliability of the electrochemical measures, each one was tested thrice, and thus, we examined the reproducibility of the results.

Table 1. Parameters for wear-corrosion tests.

Parameter	Quantity
Applied load	5 N
Velocity	50 rpm
Time of the test	60 min

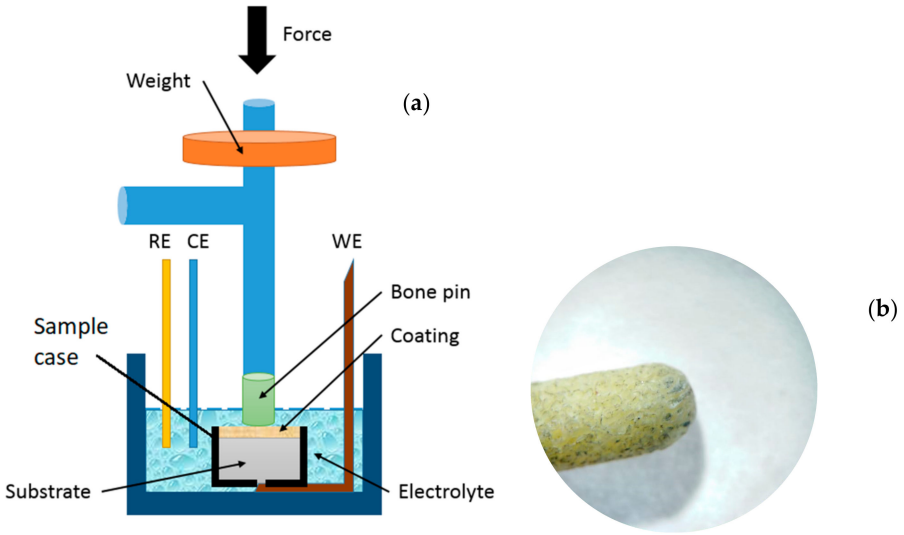

Figure 2. (**a**) Schematic model of the tribometer equipment used to make the tribocorrosion tests. (**b**) Bone pin end.

3. Results

3.1. AFM Measurements

Figure 3 shows the AFM images of the three coatings systems produced. To assess the films' surface roughness average (R_a) previously to the tribocorrosion tests, this technique was used. The Nb_2O_5 coatings presented a R_a of 18.5 nm, Nb_2O_5 + TiO_2 coatings exhibited a R_a of 36.7 nm, and finally, the TiO_2 layers showed a R_a of 29.5 nm. These are critical values for the coefficient of friction calculations in the samples and to evaluate how they influence the system response to the friction phenomena. The application of the coatings reduced the surface roughness from values around 500 nm to 40 nm in average, this is an advantage of the sputtering coatings technique. The use of a magnetron in the process guarantees high sputtered atoms density close to the substrates and thus the films homogeneity is enhanced.

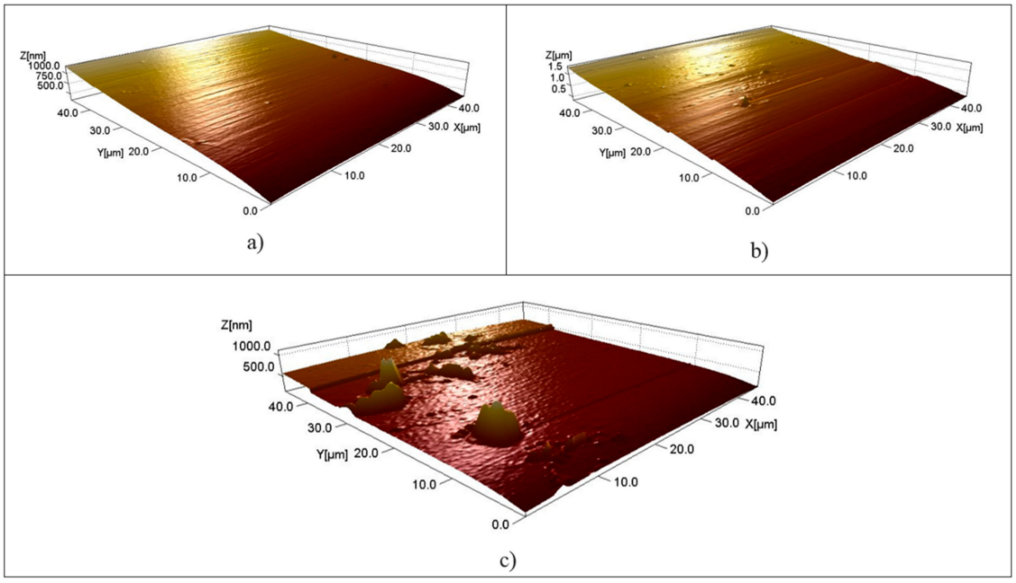

Figure 3. AFM images of the samples: (**a**) Nb_2O_5, (**b**) Nb_2O_5 + TiO_2, and (**c**) TiO_2.

3.2. Electrochemical Analysis

Figure 4 presents the experimental data of EIS tests used to determine the polarization resistance; these tests are made under a frequency swept starting from the stable potential. The polarization resistance value is obtained after adding three resistances obtained with the fit based on the equivalent circuit shown in Figure 5. These values are summarized in Table 2 for the studied coatings. Nyquist graphs allow extracting some interesting values like electrolyte resistance (R_{soln}), polarization resistance (R_{po}), and the capacitive impedance (C_c). Regarding the *n* and *m* parameters, it is evident that the systems evaluated have two CPEs (constant phase elements) in the equivalent circuit (Figure 4). In the case of the n values, the systems show a capacitive contribution without being clearly a capacitor, which gives the system corrosion resistance, as well as in the case of m parameter. The electrolyte resistance can be obtained by locating the point in which the function crosses the X axis in the Nyquist diagram. Generally speaking, R_{soln} showed similar values in all the tests demonstrating that the opposition to the mobility of the Ringer's solution ions is the same through the coatings and it is not affected with evaluation time. In Figure 4, it can be seen also that the electrical response of the coating is a double layer like the one that generates two sorts of electrical phenomena, i.e., the former at high frequencies (100 kHz to 100 Hz—response of the electrolyte in contact with the surface layer) with similar R_{po} and C_c values generating a well-defined semi-circle, and the later at low frequencies (1 Hz to 0.001 Hz—response of the substrate to coating interface), which is related to corrosion resistance values. From these results, it can be observed that TiO_2 samples offered 5.7 times higher values than the system Nb_2O_5 + TiO_2 and almost 16 times higher value than the value of the system Nb_2O_5.

Table 2. Values from the equivalent circuit fit to the electrochemical impedance spectroscopy (EIS) results in the three systems.

System	Rsoln (Ω)	Rpo (Ω)	Rcor (Ω)	Cc (µF)	n	Ccor (µF)	m
Nb_2O_5 + TiO_2	3.5	54.56	2.84	67.81	0.72	462.3	0.98
Nb_2O_5	3.1	52.8	0.40	88.44	0.76	1.041	0.97
TiO_2	3.2	63.47	16.23	69.08	0.78	69.8	0.98

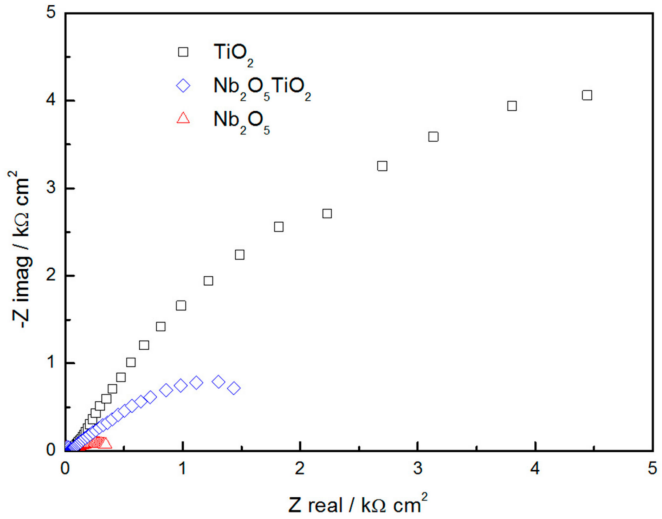

Figure 4. Nyquist graphs for the electrochemical impedance spectroscopy (EIS) tests made on the three coatings systems.

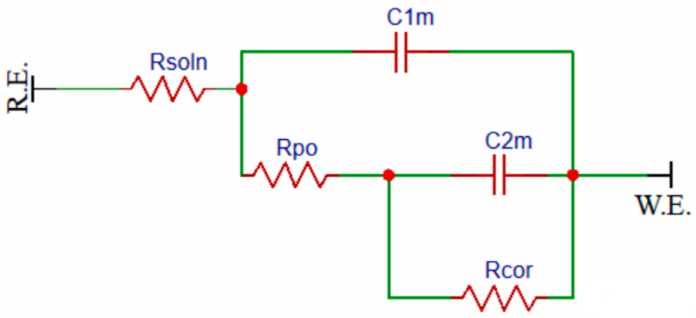

Figure 5. Equivalent electrical circuit used to simulate EIS results from Figure 3. This is a typical Randles circuit, but additionally, it has a circuit in series with coating resistance (R_{po}), which consists of a constant phase element ($C1_m$) in parallel with a resistance (R_{cor}).

In the potentiodynamic polarization results shown in Figure 6, the films named "Nb_2O_5" and "Nb_2O_5 + TiO_2" showed similar behavior in the anodic zone with comparable shape and pitting corrosion phenomena. From these curves, an increase in the corrosion current density values with low variation in corrosion potential that generates punctual anodic zones can be seen, while in the rest of the surface, there exists cathodic protection, which finally causes damage on the surface. TiO_2 coating exhibited better protection against corrosive phenomena since this compound tends to generate a passive layer, which inhibits the occurrence of degradation processes [20,21].

Nb_2O_5 sample obtained 6.562 mpy of velocity of corrosion, while a lower value of 807.7×10^{-3} mpy for the TiO_2. Due to this, corrosion potentials and current densities of the TiO_2 coating were the lower, followed by the Nb_2O_5 + TiO_2 system and finally, the Nb_2O_5 coating as can be seen in Table 3. In the mixture Nb_2O_5 + TiO_2, an intermediate behavior was observed compared to the other systems, this is attributable to the TiO_2 addition, which enhances the anticorrosive properties of the surface, and this can be evidenced with the increase on the corrosion resistance and the reduced velocity of corrosion of the mixture.

As can be seen from Table 3, there is a direct relation of the corrosion current density (I_{corr}); the lowest values were from the TiO_2 sample attributable to the excellent properties against corrosion phenomena of this material [22,23]. The sample of Nb_2O_5 + TiO_2 showed intermediate values of I_{corr}, and finally, the Nb_2O_5 sample presented the highest values from the group. The differences observed between the curves are related to the presence of titanium oxide; it was found that for the Nb_2O_5 + TiO_2 system, the I_{corr} was 2.57×10^{-6} A·cm^{-2}; for the TiO_2, this value was 9.33×10^{-7} A·cm^{-2}; and finally, for

the Nb_2O_5, it was 2.21 × 10^{-5} A·cm^{-2}. Interestingly, these coatings showed a corrosion related to the physicochemical properties of the films. Likewise, ionic conductivity is a determinant factor in the corrosion velocity values. Regarding EIS test results, TiO_2 coating is the one that presents higher corrosion resistance values; however, it is said that the ionic liberation of this is less than the rest of the studied coatings. Similarly, with the Nb_2O_5 + TiO_2 system, the TiO_2 generates a passive layer that increases solution resistance, enhancing the anticorrosive properties of the film.

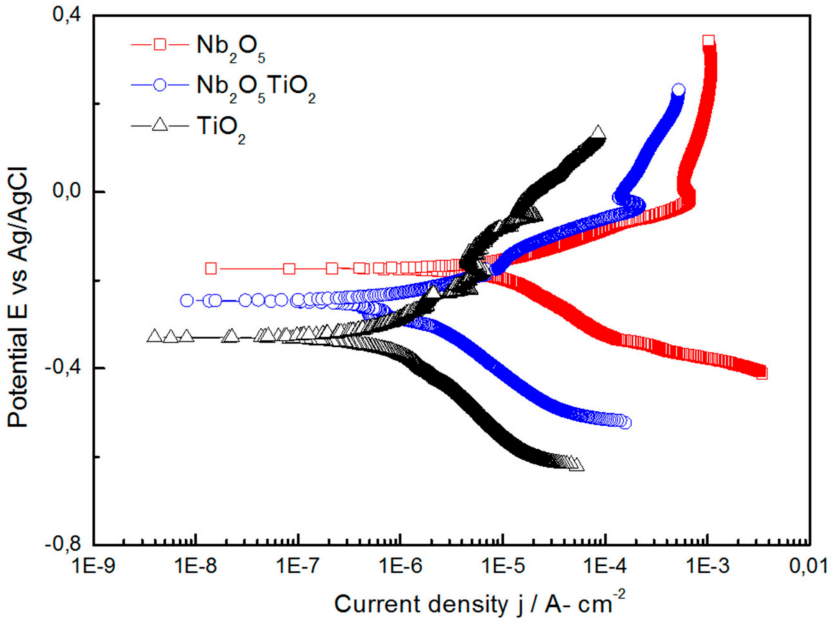

Figure 6. Potentiodynamic polarization curves for the three systems studied.

Table 3. Tafel fit values from the three systems.

System	Beta A (V/decade)	Beta C (V/decade)	E_{corr} (mV)	I_{corr} (A·cm^{-2})	V_{corr} (mpy)
Nb_2O_5	75.60 × 10^{-3}	123.0 × 10^{-3}	−0.17	2.21 × 10^{-5}	6.562
Nb_2O_5 + TiO_2	99.60 × 10^{-3}	118.9 × 10^{-3}	−0.24	2.57 × 10^{-6}	1.997
TiO_2	91.80 × 10^{-3}	154.4 × 10^{-3}	−0.33	9.33 × 10^{-7}	807.7 × 10^{-3}

Further analysis showed that for the TiO_2 coating in the anodic zone, a decrease in the corrosion current density is obtained, which generates a passivation zone, and it is present through 150 mV and after that, it is increased gradually. Generally speaking, a marked difference in terms of corrosion potential (E_{corr}) can be seen between Nb_2O_5 and TiO_2 coatings; on the one hand, the niobium oxide exhibits a higher potential or noble tendency, while on the other hand, the titanium oxide has a low potential or active tendency. However, these materials in contact with the fluid are thermodynamic unstable and thus react because of the presence of the oxide. Because it is not an equilibrium condition, the system presents a variation and hence increase the anodic voltage, and the coatings with Nb_2O_5 content exhibits a dissolution and a mass loss. Therefore, there was a significant variation on the corrosion velocity; comparing the systems, the one with high stability and with low value is the TiO_2 followed by the mixture Nb_2O_5 + TiO_2, and the one with higher degradation is the Nb_2O_5 (see Table 3) in which a susceptibility to the pitting corrosion can be observed as can be deduced from the potentiodynamic curve and the SEM images.

In the electrochemical tests of the Nb_2O_5 coatings, the results showed that the higher Rpo, the lower the corrosion rates and the better the protection. Rpo values are big for the substrates as well as for the coatings with values ranging from 6 to 170 kΩ·cm^2. These high

Rpo values of the coatings are associated with porosity probably due to the amorphous phase of the oxide film and with an effect of the electrolyte components [24]. Regarding the EIS results based on Nyquist diagram, TiO_2 system exhibited a higher capacitive capacity and a bigger impedance value. Regarding the coatings of Nb_2O_5, corrosion resistance increases due to higher impedance values explained by the formation of a stable structure that blocks the electrolyte penetration [25,26]. Comparing the values of Tables 2 and 3 corresponding to polarization resistance, it can be observed that the results are quite similar with both techniques (EIS and potentiodynamic polarization), and from this, the titanium-based coating is the one with the highest resistance against corrosion degradation among the other systems.

3.3. Coefficient of Friction and Wear Analysis

Figure 7 presents the coefficient of friction (COF) graphs for the studied systems. Sliding wear tests conditions were kept constant, the variables like traveled distance, load, and temperature were replicated for the three coatings systems. Nb_2O_5 sample shows the running-in process that is related to the variation of the coating surface in the first minutes of the test due to interface contact. Based on the interpretation of the coefficient of friction presented by Blau et al., the behavior of this coating was identified [27]. The increase in the COF is attributed to the coating wear, which causes particles liberation that generates a third body in contact and thus influences the tribological pair creating a fast friction transition that causes high increase in COF [27,28].

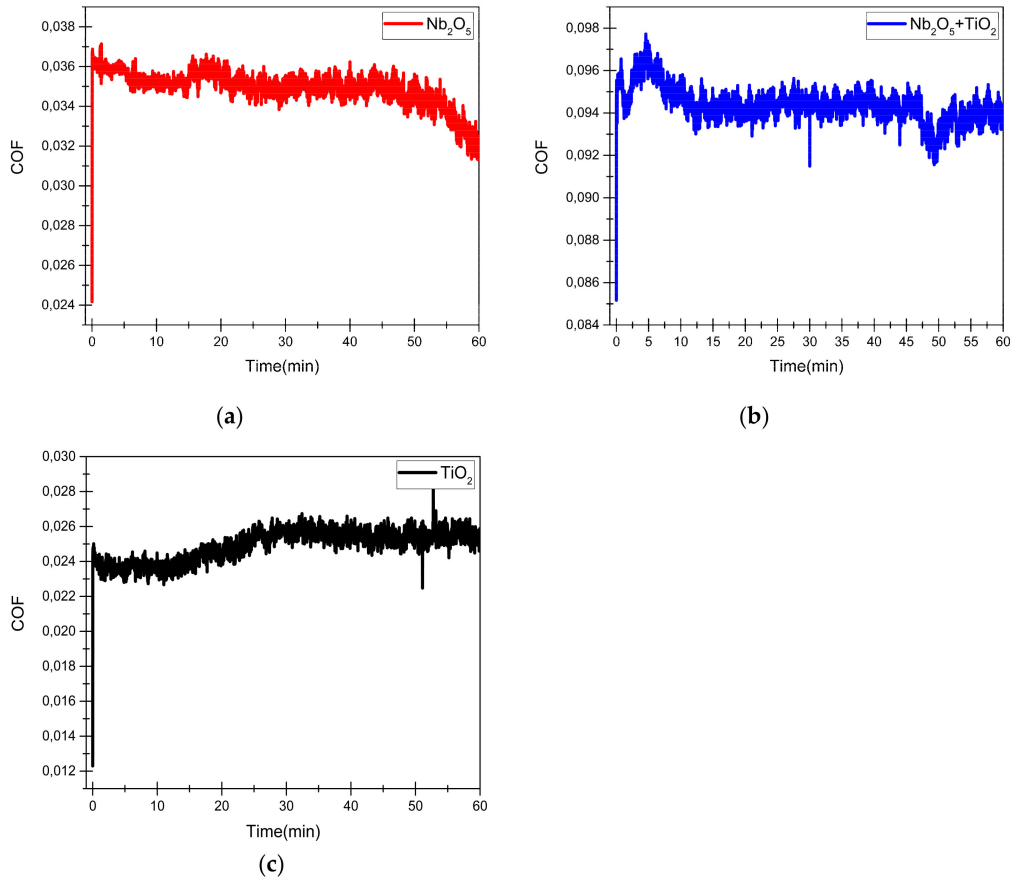

Figure 7. Coefficient of friction for the three systems studied: (**a**) Nb_2O_5, (**b**) Nb_2O_5 + TiO_2, and (**c**) TiO_2.

Regarding Nb_2O_5 + TiO_2 sample, a variation in the COF magnitude was observed, and a start period exists and is associated to the friction mechanism of interference due to the contact between the tips of the harshness of both bodies, i.e., the bone pin and the

coating surface. By increasing test time, the harshness is smoothed, and a passive layer is generated reducing COF values [27–29], however, COF value is intermediate among the other coatings, and it is related with this coating roughness obtained by means of AFM technique. In the final part of the test for this coating, an increase in COF values can be seen and is attributable to the detachment of the passive layer and the start of the pitting corrosion, which degrades the surface in punctual zones. This system presented an intermediate behavior for the corrosion resistance as well as wear.

Finally, for TiO_2 coating, the COF behavior shows a running-in process at the beginning (first 10 min) since the initial contacts that are bonded with the attraction forces between bone molecules and coatings surface must be broken. The presented range is denominated as static wear. After this point, it can be determined that COF decreases under the static value so that kinetic coefficient is less than the static one and kept constant after 25 min indicating the reach of the stationary state. In this TiO_2 coatings, adhesive wear was evidenced by means of SEM (scanning electron microscopy) images, this degradation causes the concentration of strains around the bone pin contact zones that causes detachment of some coatings surface zones.

In Figure 8, there is an apparent similar behavior between Nb_2O_5 and Nb_2O_5 + TiO_2 samples where pitting corrosion is evidenced, nevertheless the addition of TiO_2 in the mixture coating (Figure 7b) helps to protect its surface as the number of pitting marks is highly reduced and thus the surface damage.

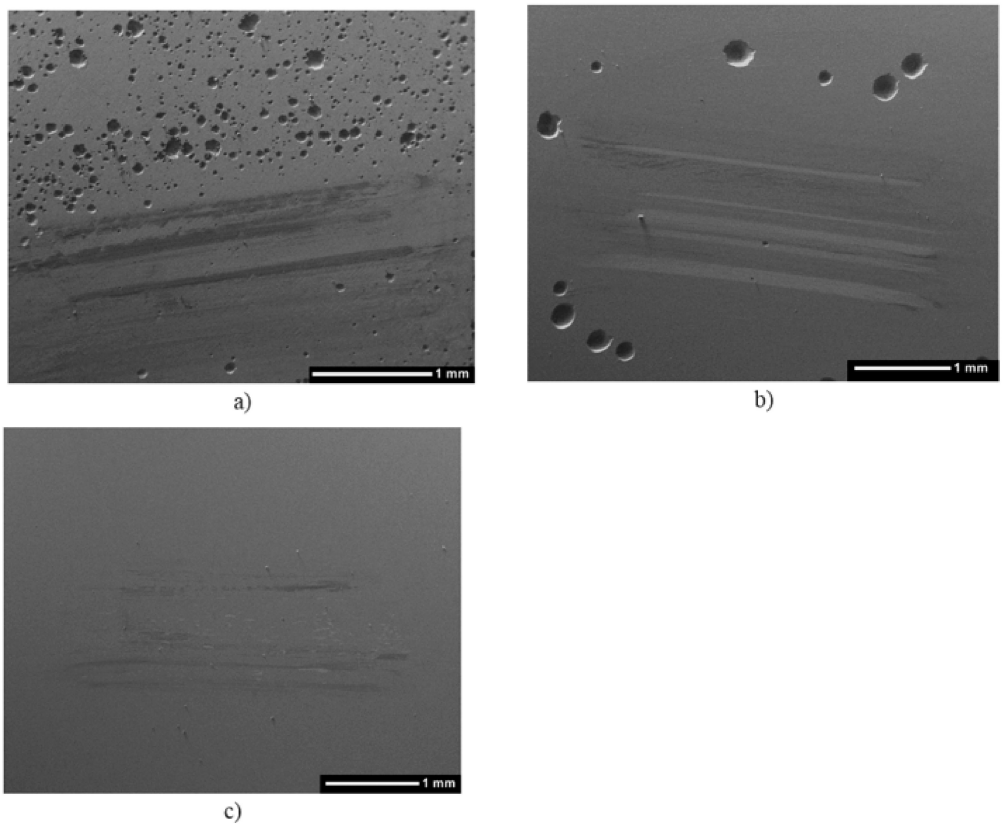

Figure 8. SEM micrographs for the three systems evaluated, taken at 30× magnification: (**a**) Nb_2O_5 (**b**) Nb_2O_5 + TiO_2, and (**c**) TiO_2.

SEM micrographs also show the deterioration of the coatings surface for all the systems Nb_2O_5, TiO_2, and Nb_2O_5 + TiO_2 related to the tribocorrosion phenomena. On the surfaces, adhesive wear was observed for all the coatings systems in which a displacement of material through the wear track edge is generated. Figure 9 shows 300× SEM micrographs of the coatings surface in the wear track zone; samples of Nb_2O_5 and Nb_2O_5 + TiO_2 presented plough lines characteristic for this wear phenomena as shown in the figure. TiO_2

sample exhibited adhesive wear evidenced by the detachment of the thin films in some specific zones.

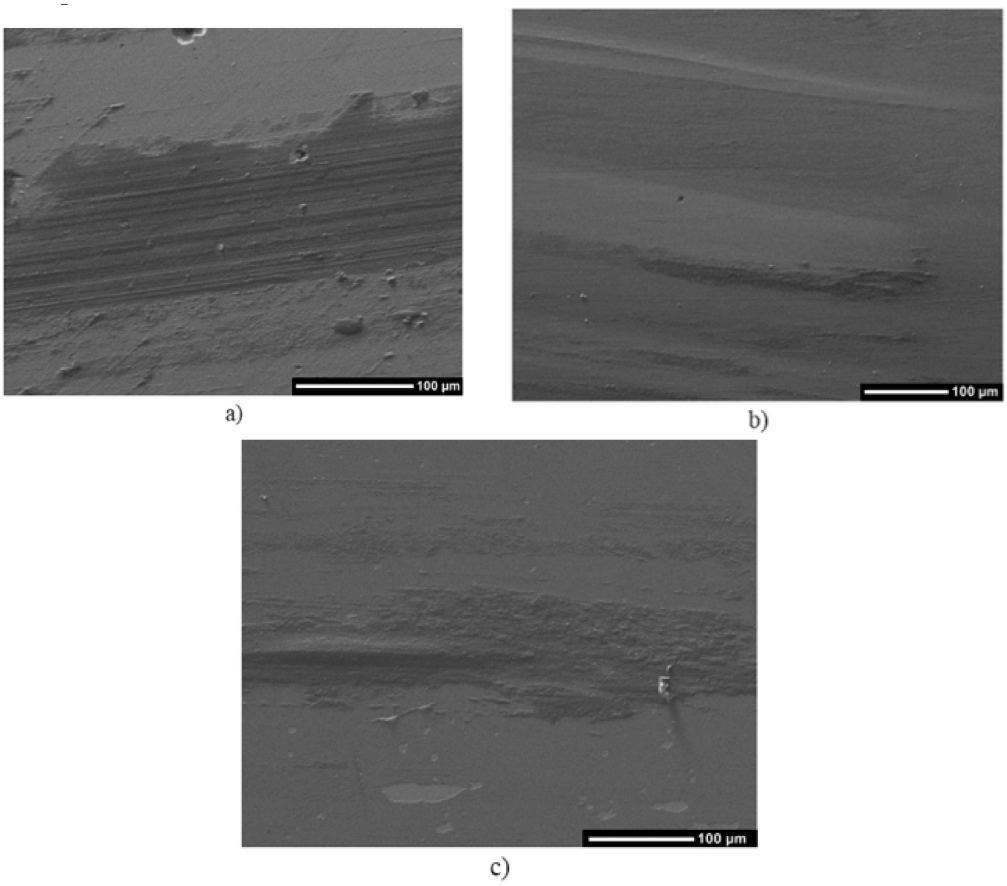

Figure 9. SEM micrographs for the three systems evaluated, taken at 300× magnification: (**a**) Nb_2O_5, (**b**) Nb_2O_5 + TiO_2, and (**c**) TiO_2.

4. Conclusions

The analysis of EIS results has shown that the TiO_2 sample presented the best behavior among the rest of the systems, this is evidenced by the semicircles presented in Nyquist diagrams, and this is also related to the porosity of the material. For TiO_2, the potentiodynamic polarization results analyzed by Tafel extrapolation are in accordance with the ones of EIS tests and thus the good behavior against corrosion resistance.

Although for all the coating systems studied in this paper the tribocorrosion tests were made keeping the conditions as constant, the running-in process was evident among all of them and is related to the obtained roughness by AFM and the COF values. High surface roughness values increase the COF values because of the interaction forces between the bone pin and coating surface. The best behavior was shown by the Nb_2O_5 coating followed by the mixture Nb_2O_5 + TiO_2 and finally the TiO_2 one.

The Nb_2O_5 sample tends to present a better behavior against wear phenomena, however, against corrosion ones, it degrades by pitting. Contrary, the TiO_2 sample presents a better corrosion resistance as it does not present the pitting process; however, against wear phenomena, it degrades and exhibits zones with adhesive wear and film detachment. Finally, the mixed sample Nb_2O_5 + TiO_2 showed an intermediate behavior in which regarding wearing it does not degrade like TiO_2 film nevertheless suffer some pitting processes on the surface that are not quite severe as the ones presented by Nb_2O_5 film.

Author Contributions: Conceptualization, W.A., P.G.D. and G.O.-H.; methodology, W.A., P.G.D. and G.O.-H.; formal analysis, W.A., P.G.D. and G.O.-H.; investigation, W.A., P.G.D. and G.O.-H. All authors have read and agreed to the published version of the manuscript.

Funding: This research was funded by Universidad Militar Nueva Granada, project number IMP ING 3123.

Institutional Review Board Statement: Not applicable.

Informed Consent Statement: Not applicable.

Data Availability Statement: Not applicable.

Acknowledgments: W.A. thanks the Vicerectoria de investigaciones Universidad Militar Nueva Granada Project IMP ING 3123 validity 2020–2021.

Conflicts of Interest: The authors declare no conflict of interest. The funders had no role in the design of the study; in the collection, analyses, or interpretation of data; in the writing of the manuscript; or in the decision to publish the results.

References

1. Sarmiento-González, A.; Encinar, J.R.; Marchante-Gayón, J.M.; Sanz-Medel, A. Titanium levels in the organs and blood of rats with a titanium implant, in the absence of wear, as determined by double-focusing ICP-MS. *Anal. Bioanal. Chem.* **2009**, *393*, 335–343. [CrossRef] [PubMed]
2. Ramírez, G.; Rodil, S.E.; Arzate, H.; Muhl, S.; Olaya, J.J. Niobium based coatings for dental implants. *Appl. Surf. Sci.* **2011**, *257*, 2555–2559. [CrossRef]
3. Niinomi, M.; Nakai, M.; Hieda, J. Development of new metallic alloys for biomedical applications. *Acta Biomater.* **2012**, *8*, 3888–3903. [CrossRef] [PubMed]
4. Li, Y.; Munir, K.S.; Lin, J.; Wen, C. Titanium-niobium pentoxide composites for biomedical applications. *Bioact. Mater.* **2016**, *1*, 127–131. [CrossRef]
5. Ou, K.L.; Weng, C.C.; Lin, Y.H.; Huang, M.S. A promising of alloying modified beta-type Titanium-Niobium implant for biomedical applications: Microstructural characteristics, in vitro biocompatibility and antibacterial performance. *J. Alloys Compd.* **2017**, *697*, 231–238. [CrossRef]
6. Gabriel, S.B. Characterization of a new beta titanium alloy, Ti–12Mo–3Nb, for biomedical applications. *J. Alloys Compd.* **2012**, *536*, S208–S210. [CrossRef]
7. Latchford, I.; Riposan, A.; Kudiravstev, V.; Bluck, T.; Smith, C. Cost of ownership analysis for high productivity thin film PVD system. In Proceedings of the 2014 Technical Conference, Philadelphia, PA, USA, 19–20 June 2014; Society of Vacuum Coaters: Albuquerque, NM, USA, 2014.
8. Chen, W.A. A market analysis for PVD coating system of by project submitted in partial fulfillment. Master's Thesis, Simon Fraser University, Burnaby, BC, Canada, 2012.
9. Ibrahim, Z.; Sarhan, A.D.; Yusuf, F.; Hamdi, M. Biomedical materials and techniques to improve the tribological, mechanical and biomedical properties of orthopedic implants—A review article. *J. Alloys Compd.* **2017**, *714*, 636–667. [CrossRef]
10. Yanisarapan, T.; Thunyakitpisal, P.; Chantarawaratit, P. Corrosion of metal orthodontic brackets and archwires caused by fluoride-containing products: Cytotoxicity, metal ion release and surface roughness. *Orthod. Waves.* **2018**, *77*, 79–89. [CrossRef]
11. Hasegawa, M.; Wakabayashi, H.; Sudo, A. A case of bone necrosis with pseudotumor following metal-on-metal total hip arthroplasty. *Arthroplast. Today* **2017**, *4*, 291–294. [CrossRef]
12. Li, J.J.; Sydney, N.; Health, L.; Leonards, S. *Tissue Response to Biomaterials*; Elsevier Inc.: Amsterdam, The Netherlands, 2018.
13. Eisenbarth, J.B.E.; Velten, D.; Müller, M.; Thull, R. Nanostructured niobium oxide coatings influence osteoblast adhesion. *Clin. Exp. Rheumatol.* **2015**, *33*, 97–103. [CrossRef]
14. Sowa, M.; Greń, K.; Kukharenko, A.I.; Korotin, D.M.; Michalska, J.; Szyk-Warszyńska, L.; Mosiałek, M.; Zak, J.; Pamuła, E.; Kurmaev, E.Z.; et al. Influence of electropolishing and anodic oxidation on morphology, chemical composition and corrosion resistance of niobium. *Mater. Sci. Eng. C* **2014**, *42*, 529–537. [CrossRef]
15. Pauline, S.A.; Rajendran, N. Corrosion behaviour and biocompatibility of nanoporous niobium incorporated titanium oxide coating for orthopaedic applications. *Ceram. Int.* **2017**, *43*, 1731–1739. [CrossRef]
16. Kumar, P.; Duraipandy, N.; Manikantan Syamala, K.; Rajendran, N. Antibacterial effects, biocompatibility and electrochemical behavior of zinc incorporated niobium oxide coating on 316L SS for biomedical applications. *Appl. Surf. Sci.* **2018**, *427*, 1166–1181. [CrossRef]
17. Rodriguez-Barrero, S.; Fernández-Larrinoa, J.; Azkona, I.; López de la calle, L.N.; Polvorosa, R. Enhanced performance of nanostructured coatings for drilling by droplet elimination. *Mater. Manuf. Process.* **2016**, *31*, 593–602. [CrossRef]
18. Polvorosa, R.; Suárez, A.; López de la calle, L.N.; Cerillo, I.; Wretland, A.; Veiga, F. Tool wear on nickel alloys with different coolant pressures: Comparison of Alloy 718 and Waspaloy. *J. Manuf. Process.* **2017**, *26*, 44–56. [CrossRef]
19. Bono, J.V.; McCarthy, J.C. *Revision Total Hip Arthroplasty*; Springer: New York, NY, USA, 1999.

20. Luo, Y.; Yang, L.; Tian, M. 3-Application of biomedical-grade titanium alloys in trabecular bone and artificial joints Biomaterials and Medical Tribology. In *Woodhead Publishing Series in Biomaterials*; Woodhead Publishing: Cambridge, UK, 2013; pp. 181–216.
21. Bait, L.; Azzouz, L.; Madaoui, N.; Saoula, N. Influence of substrate bias voltage on the properties of TiO2 deposited by radio-frequency magnetron sputtering on 304L for biomaterials applications. *Appl. Surf. Sci.* **2017**, *395*, 72–77. [CrossRef]
22. Yetim, T. An investigation of the corrosion properties of Ag-doped TiO2-coated commercially pure titanium in different biological environments. *Surf. Coat. Technol.* **2017**, *309*, 790–794. [CrossRef]
23. Devikala, S.; Kamaraj, P.; Arthanareeswari, M. Corrosion resistance behavior of PVA/TiO_2 composite in 3.5% NaCl. *Mater. Today Proc.* **2018**, *5*, 8672–8677. [CrossRef]
24. Rojas, P.N.; Rodil, S.E. Corrosion behavior of amorphous niobium oxide coatings. *Int. J. Electrochem. Sci.* **2012**, *7*, 1443–1458.
25. Wang, H.; Zang, R.; Yuan, Z.; Shu, X.; Liu, E.; Han, Z. A comparative study of the corrosion performance of titanium (Ti), titanium nitride (TiN), titanium dioxide (TiO_2) and nitrogen-doped titanium oxides (N–TiO2), as coatings for biomedical applications. *Ceram. Int.* **2015**, *41*, 11844–11855. [CrossRef]
26. Yetim, T. Corrosion behavior of Ag-doped TiO2 coatings on commercially pure titanium in simulated body fluid solution. *J. Bionic Eng.* **2016**, *13*, 397–405. [CrossRef]
27. Blau, P.J. On the nature of running-in. *Tribol. Int.* **2005**, *38*, 1007–1012. [CrossRef]
28. Blau, P. *Friction Science and Technology*; CRC Press: Boca Raton, FL, USA, 2008; Volume 20084465.
29. Vieira, A.C.; Ribeiro, A.R.; Rocha, L.A.; Celis, J.P. Influence of pH and corrosion inhibitors on the tribocorrosion of titanium in artificial saliva. *Wear* **2006**, *261*, 994–1001. [CrossRef]